Article
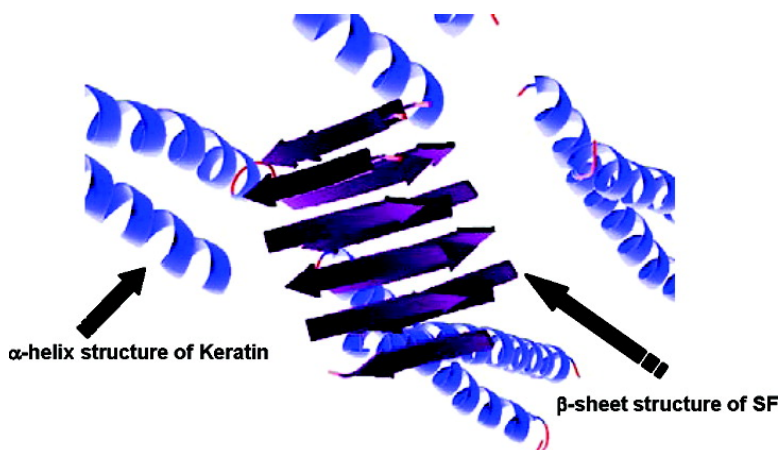
Biodegradable Materials Based on Silk Fibroin and Keratin

Andreia Vasconcelos, Giuliano Freddi, and Artur Cavaco-Paulo

α-helix structure of Keratin

β-sheet structure of SF

More About This Article

Additional resources and features associated with this article are available within the HTML version:

- Supporting Information
- Access to high resolution figures
- Links to articles and content related to this article
- Copyright permission to reproduce figures and/or text from this article

View the Full Text HTML

Biodegradable Materials Based on Silk Fibroin and Keratin

Andreia Vasconcelos,[†] Giuliano Freddi,[†,‡] and Artur Cavaco-Paulo*,[†]

*University of Minho, Campus de Azurém, 4800-058 Guimarães, Portugal, Silk Research Institute,
via Giuseppe Colombo 83, 20133 Milan, Italy*

Wool and silk were dissolved and used for the preparation of blended films. Two systems are proposed: (1) blend films of silk fibroin and keratin aqueous solutions and (2) silk fibroin and keratin dissolved in formic acid. The FTIR spectra of pure films cast from aqueous solutions indicated that the keratin secondary structure mainly consists of α-helix and random coil conformations. The IR spectrum of pure SF is characteristic of films with prevalently amorphous structure (random coil conformation). Pure keratin film cast from formic acid shows an increase in the amount of β-sheet and disordered keratin structures. The FTIR pattern of SF dissolved in formic acid is characteristic of films with prevalently β-sheet conformations with β-sheet crystallites embedded in an amorphous matrix. The thermal behavior of the blends confirmed the FTIR results. DSC curve of pure SF is typical of amorphous SF and the curve of pure keratin show the characteristic melting peak of α-helices for the aqueous system. These patterns are no longer observed in the films cast from formic acid due to the ability of formic acid to induce crystallization of SF and to increase the amount of β-sheet structures on keratin. The nonlinear trend of the different parameters obtained from FTIR analysis and DSC curves of both SF/keratin systems indicate that when proteins are mixed they do not follow additives rules but are able to establish intermolecular interactions. Degradable polymeric biomaterials are preferred candidates for medical applications. It was investigated the degradation behavior of both SF/keratin systems by in vitro enzymatic incubation with trypsin. The SF/keratin films cast from water underwent a slower biological degradation than the films cast from formic acid. The weight loss obtained is a function of the amount of keratin in the blend. This study encourages the further investigation of the type of matrices presented here to be applied whether in scaffolds for tissue engineering or as controlled release drug delivery vehicles.

1. Introduction

Keratin is the major structural fibrous protein providing outer covering such as hair, wool, feathers, nails, and horns of mammals, reptiles, and birds.[1] At the molecular level, the most distinctive feature is the high concentration in cysteine residue (7−20 number % of the total amino acid residues).[2] These cysteine residues are oxidized to give inter- and intramolecular disulfide bonds, which decide about mechanical, thermal, and chemical properties of wool fibers. Wool keratins are a family of proteins that can be roughly classified into two groups: the intermediate filament proteins (IFPs) and the matrix proteins.

The most abundant are the fibrous, low-sulfur keratins that are part of the IFPs. They have a α-helical tertiary structure and have an average molar mass in the range of 40–60 kDa. The matrix proteins have a high content in either cysteine or glycine and tyrosine residues. The ones with high cysteine content are referred to as the high-sulfur proteins (HSPs) and have a molecular weight in the range of 11–26 kDa. Those high in glycine and tyrosine residues are referred to as high-glycine/tyrosine proteins (HGTPs) and have a molecular weight between 6 and 9 kDa. The matrix proteins are thought to surround the IFPs and interact with them through intermolecular disulfide bonds.[3]

The keratin macromolecule in wool fiber takes the following conformations: helical (α-keratin), rectal (β-keratin), and undefined. The α-helix conformation is characteristic for wool fiber in its native state, that is, the fiber that is not stretched along its axis.[4] During stretching, the α-helix declines and β-keratin appears. It is an unstable conformation, and when the stretching force disappears, the conformation of keratin reverts to α-helical.[5–7]

Extraction of keratins from wool has been conducted in various ways,[8–15] but all of them involve the presence of reducing or denaturant agents to break disulfide bonds. Regenerated keratin from wool is then dissolved in proper solvents before processing into other applications. Although regenerated keratin has been used for many applications,[16] this material presents poor mechanical strength so that the use of cross-linking agents and blending with structural fibrous polymers is often necessary to improve its processing and final mechanical properties. Regenerated keratin blended with silk fibroin has already been reported,[17] and formic acid represents an ideal medium for this polymer blend because while wool is partially soluble in formic acid, regenerated keratin and silk fibroin are readily soluble.[18,19]

Silk from silkworms and orb-weaving spiders represent a unique family of structural proteins that are biocompatible, degradable, mechanically superior, offer a wide range of properties such as environmental stability, controlled proteolytic biodegradability, morphologic flexibility, and can be chemically modified to suit a wide range of biomedical applications.[20–32]

The silk fibers from silkworm *Bombyx mori* consist of two proteins: a light chain ($\cong$25 kDa) and a heavy chain ($\cong$390 kDa), which are present in a 1:1 ratio and linked by a single disulphide bond.[33] These proteins are coated with a family of hydrophilic proteins called sericins (20–310 kDa),[33–36] and

* Corresponding author. E-mail: artur@det.uminho.pt (A.C.-P.); andreiav@det.uminho.pt (A.V.).
† University of Minho.
‡ Silk Research Institute.

25–30% of a silk cocoon's mass is sericin that is removed during the degumming process.

The amino acid composition of silk fibroin from *B. mori* consists primarily of glycine, alanine, and serine amino acids in the molar ratio of 3:2:1 which forms typical −(−ala−gly−)$_n$− repeating motifs[34]. In the fiber, fibroin chains are aligned along the fiber axis held together by a close network of interchain hydrogen bonds with adjacent −(−ala−gly−)$_n$− sequences forming the well-known β-sheets crystals.[33,37]

Both keratin and fibroin are excellent biopolymers with outstanding properties that make them extremely valuable in biomedical field. Keratin films prepared from reduced keratin are biodegradable in vivo and in vitro,[38] supporting cell adhesion and proliferation.[16,39] Silk fibroin films that are easily prepared by casting aqueous silk proteins solutions at room temperature are highly attractive for their discrete permeability to oxygen and water vapor.[40,41] Silk fibroin has also been used for the preparation of polymer−hydroxyapatite composites for bone regeneration,[42] wire ropes for the substitution of the anterior cruciate ligament,[43] and novel silk-based sutures and protective gauzes for the treatment of skin burns with improved blood compatibility[44] for supporting cell adhesion and growth, as scaffolds for skin and bone regeneration.[45−48]

In the present work, blend films of silk fibroin from *B. mori* and regenerated keratin from merino wool were prepared by water and formic acid casting and characterized in the solid state by FT-IR spectroscopy, DSC thermal analysis, and tensile measurements. The corresponding solutions were characterized by amino acid analysis and SDS-PAGE electrophoresis.

2. Materials and Methods

2.1. Preparation of Stock Solutions. Silk fibroin, SF, 1% (w/v) (SF1) was prepared by dissolving 1 g of degummed silk fibers into 10 mL of saturated aqueous LiBr (catalogue no. P5147, Sigma, MO) at 60 °C for 3 h. The solution was then diluted by adding 90 mL of deionized water, filtered, and dialyzed against distilled water until complete removal of salt, using cellulose tubing (molecular-weight cutoff of 12000–14000 Da). A similar solution was prepared in the same manner that was then freeze-dried (SF2).

Keratin 1% (w/v) (K1) solution was prepared by immersing 1 g of delipided wool in 10 mL of a solution containing 8 M urea (catalogue no. U5378, Sigma, Spain), 0.2 M SDS (catalogue no. L4390, Sigma, Spain) and 0.5 M $Na_2S_2O_5$ (catalogue no. 31448, Sigma, Spain). The mixture was heated to 100 °C for 30 min. The solution was then diluted with 90 mL of distilled water, filtered, and dialyzed against distilled water using cellulose tubing (molecular-weight cutoff of 12000–14000 Da).

Delipided wool (1 g) was dissolved in 25 mL of a solution containing 0.1 M Tris-HCl, pH 9.0, 8 M urea and 0.1 M DTT (catalogue no. D9779, Sigma, Spain) at 50 °C for 24 h in a shaker bath. The solution was filtered and dialyzed against distilled water using cellulose tubing (molecular-weight cutoff of 12000–14000 Da). After dialysis the solution was freeze-dried (K2).

2.2. Preparation of Blended Films. Keratin (K1) and silk fibroin (SF1) solutions (10 mL of final volume) were blended in the ratios of 80/20, 60/40, and 40/60 of SF1/K1. The blends were cast in plastic Petri dishes with a circular area of about 40 cm^2 and dried at room temperature. The controls are 100% SF1 and 100% K1.

Freeze-dried keratin (K2) and silk fibroin (SF2) were dissolved in formic acid to prepare 1% (w/v) solutions. The solutions were blended in the ratios of 75/25, 50/50, and 25/75 of SF2/K2. The blends were cast in plastic Petri dishes with a circular area of about 40 cm^2 and dried at room temperature. The controls are 100% SF2 and 100% K2. The resulting films were 0.03 mm in average thickness.

2.3. Amino Acid Analysis. The amino acid composition of keratin and silk fibroin samples was determined after acid hydrolysis with 6

Table 1. Amino Acid Composition of Silk Fibroin and Keratin

amino acid	silk fibroin (mol %)	keratin (mol %)
Cyst		0.46
Asp	−1.67	5.94
Ser	11.48	10.77
Glu	1.37	10.96
Gly	43.68	11.02
His	0.20	1.00
Arg	0.62	5.55
Thr	0.96	5.12
Ala	29.34	4.52
Pro	0.67	7.06
Cys	0.10	9.09
Tyr	5.30	6.26
Val	2.23	5.29
Met	0.10	0.37
Lys	0.33	1.17
Ile	0.66	3.06
Leu	0.58	8.46
Phe	0.72	3.88

N HCl at 105 °C for 24 h under vacuum. Free amino acids analyzed by HPLC according to the AccQ-Tag method (Waters). The eluate was detected at 254 nm. Samples were analyzed in duplicate (error: ±2%). The quantitative amino acid composition, expressed as mol % for each amino acid, was determined by external standard calibration (Amino Acid Standard H, Pierce).

2.4. SDS-PAGE. SDS-PAGE was carried out using the Mini-PROTEAN 3 Cell system from Bio-Rad. The resolving gels (15% acrylamide of about 0.75 mm thickness) were run at a constant voltage (170 V) and prepared according to the method described by Laemmli.[49] Proteins were visualized by Coomassie Brilliant blue G 250 staining using phosphorylase-b (97 kDa), albumin (66 kDa), ovalbumin (45 kDa), carbonic anhydrase (30 kDa), trypsin inhibitor (20.1 kDa) and α-lactalbumin (14.4 kDa) for calibration.

2.5. FT-IR Spectroscopy. FT-IR spectra of controls and blended SF1/K1 and SF2/K2 films were measured with a Nicolet FT-IR Nexus spectrometer (Thermo Scientific) equipped with a ZnSe ATR cell (model Smart Performer). The analysis was performed in triplicate.

2.6. Thermal Analysis. Differential scanning calorimetry (DSC) measurements were performed with a DSC-30 instrument (Mettler Toledo) from room temperature to 120 °C at a heating rate of 10 °C/min and kept at 120 °C for 10 min to induce dehydration of samples. The temperature was lowered to room temperature and increased to 500 °C at a heating rate of 10 °C/min. Sample weight was 2–3 mg. The open aluminum cell was swept with N_2 during the analysis.

2.7. Mechanical Properties. Mechanical properties of a film strip with 1 cm width were measured using an Instron dynamometer model 5500 with a 30 mm gauge length at a crossbar rate of 15 mm/min, corresponding to a strain rate of $1.0 \times 10^{-2} \text{ s}^{-1}$. The analysis was performed in triplicate.

2.8. In Vitro Degradation. Protein matrices were incubated at 37 °C in 6 mL of a solution containing 0.5 mg/mL of trypsin (from porcine pancreas, catalogue no. T7409, Sigma, Spain) in phosphate-buffered saline (PBS) or in PBS as a control. Before incubation with trypsin, SF1/K1 films were treated with 90% (v/v) of methanol (catalogue no. 179337, Sigma, Spain) during 1 h at room temperature. The SF2/K2 films were directly used for the degradation studies.

Solutions were changed and collected daily. At designated time points, samples were washed thoroughly with distilled water, dried in a desiccator, and weighed to estimate the extent of degradation.

3. Results and Discussion

3.1. Amino Acid and SDS-PAGE Results. The protein solutions of wool keratin and silk fibroin were characterized by amino acid analysis and SDS-PAGE electrophoresis. Amino acid analysis on Table 1 indicated that the cysteine residues
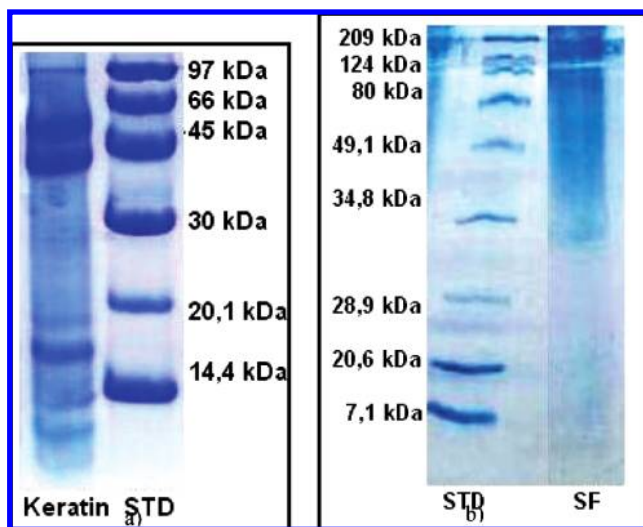
Figure 1. SDS-PAGE of (a) wool keratin and (b) silk fibroin solutions.

Table 2. Mechanical Properties of SF1/K1 Blends

K1 (%)	stress (MPa)	elongation (mm)	modulus (MPa)
0	23.690 ± 7.311	0.518 ± 0.0416	3411 ± 479
20	11.265 ± 5.167	0.679 ± 0.1948	1597 ± 588
40	9.153 ± 3.250	0.407 ± 0.1135	1409 ± 203

Table 3. Mechanical Properties of SF2/K2 Blends

K2 (%)	stress (MPa)	elongation (mm)	modulus (MPa)
0	23.568 ± 7.669	0.427 ± 0.051	2893 ± 387
25	29.755 ± 6.544	0.570 ± 0.130	2724 ± 207
50	17.730 ± 4.660	0.363 ± 0.111	2005 ± 210

occupied 8–9 mol % of the total amino acid residues of the reduced keratin as already described before.[50,51] The amino acid composition of SF is characterized by a high content of Gly, Ala, and Ser, which total about 85 mol %, Tyr accounts for 5.3 mol %, and acidic and basic amino acids total about 3.0 and 1.1 mol %, respectively. This characteristic amino acidic pattern results from the contribution of two polypeptides, i.e., the heavy and light chains. The heavy chain represents about 90% of the total weight of silk fibroin and predominates with its characteristic $-(Gly-Ala)_n-$ rich sequences[33] over the more heterogeneous primary structure of the light chain.[35]

The electrophoretic pattern of wool keratin (Figure 1) shows the main two groups of keratin associated proteins, the intermediate filament proteins (IFPs), and the matrix proteins. It can be observed (Figure 1a) two high-molecular-weight bands (60–45 kDa) attributed to the low-sulfur IFPs that are mainly α-helical, and several low-molecular-weight bands attributed to the high-sulfur (HSPs) (20−10 kDa) and high-glycine/tyrosine (HGTPs) (6–9 kDa) proteins of the matrix.[3]

Regenerated aqueous SF solution (Figure 1b) shows a broad dull band from 200–30 kDa and a very weak band at approximately 25 kDa.[52] The former band might result from the degradation products of the heavy chains (350 kDa) of raw silk protein formed by degumming and dissolution in a solvent system, and the latter band at 25 kDa corresponds to the light chain of raw silk protein.[53]

Keratin was extracted from wool by sulfitolysis.[54,55] During this process. cysteine disulphide bonds are cleaved by sulfite to give cysteine thiol (reduced keratin) and Bunte salts residues.[56] This method gives a keratin extraction yield about 30% of the total protein content of the original wool.[57]

Keratin extracted by the system using DTT as the reducing agent gives a protein extraction yield of approximately 80%.[58] However, the solution obtained by this method became partially insoluble after dialysis. This is due to the fact that the high-sulfur proteins responsible for the reoxidation of the SH groups into disulphide bridges are insoluble. The SDS-PAGE gel shows that the HSPs (20–10 kDa) remains in the insoluble fraction of the solution. In the protein solution obtained by sulfitolysis, this fact is not observed because these type of proteins are not extracted by this method (data not shown). In terms of processing, this fact is an advantage because the solution is ready for film preparation but the films obtained have low mechanical

strength when compared with the films obtained by formic acid casting (Table 3).

3.2. Mechanical Properties Results. The load/elongation curves of pure SF1 films (data not shown) do not show any yield point. The load increases almost linearly until a plateau, then the film brakes or continues elongating (failure is not sharp). These SF1 films are prevalently amorphous. The tensile behavior can be due to the presence of amorphous domains that display a plastic behavior. Addition of keratin (K1) to SF1 makes films weaker. The average values of stress are about half of those of pure SF1 films when 40% of K1 is present. Elasticity increases slightly at small keratin content (Table 2).

SF films cast from formic acid (SF2) display average stress values similar to water cast films, but failure is much sharper. This can be attributed to the more crystalline character of these films. The SF2/K2 films obtained with formic acid display better tensile properties than those obtained in water. At 50% of K2, the tensile behavior is typical of brittle films, and the failure is sharp. At lower K2 content (25%), failure can be sharp or plastic. It is important to note that the stress values are quite high, similar to those of pure SF2 films (Table 3).

3.3. FT-IR Results. Infrared absorption spectra of blended films of silk fibroin (SF1 and SF2) and keratin (K1 and K2) show characteristic absorption bands assigned to the peptide bonds $(-CONH-)$ that originate bands known as amide I, amide II, and amide III.

Amide I is useful for the analysis of the secondary structure of the proteins and is mainly related with the $C=O$ stretching, and it occurs in the range of 1700–1600 cm^{-1}. Amide II, which falls in 1540–1520 cm^{-1} range, is related with the N−H bending and C−H stretching vibration. Amide III occurs in the range of 1220–1300 cm^{-1}, and it results from in phase combination of C−N stretching and $C=O$ bending vibration.[59] In addition, the positions of these bands indicate the conformations of the protein materials: 1650 cm^{-1} (random coil) and 1630 cm^{-1} (β-sheet) for amide I, 1540 cm^{-1} (random coil) and 1520 cm^{-1} (β-sheet) for amide II, and 1230 cm^{-1} (random coil) and 1270 cm^{-1} (β-sheet) for amide III.[60–62]

The keratin (K1) spectra (Figure 2) shows a peak at 1641 cm^{-1} with a shoulder at about 1620 cm^{-1} for amide I, 1533 cm^{-1} amide II, and 1225 cm^{-1} for amide III. The peaks at 1203 and 1024 cm^{-1} are related, respectively, to the asymmetric and symmetric S−O stretching vibrations of the Bunte salts residues[63] that are no longer observed in the spectra of K2 (Figure 4). The absorption value of the amide I band of pure K1 film indicates that the secondary structure of K1 mainly consist of α-helix and random coil conformation The IR spectra of SF showed a peak at 1639 cm^{-1} for amide I, 1518 cm^{-1} with a strong shoulder at about 1535 cm^{-1} for amide II, and 1236 cm^{-1} for amide III. This FTIR pattern is characteristic of SF films with prevalently amorphous structure (random coil/silk I
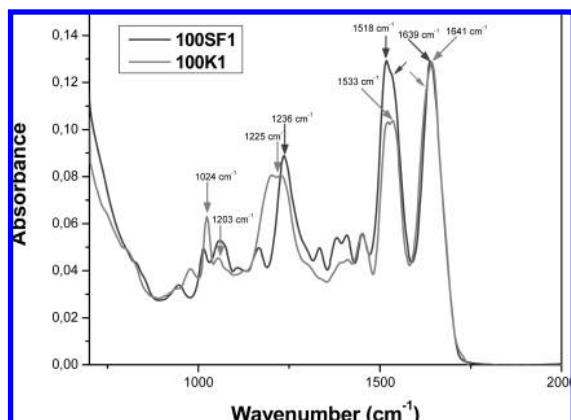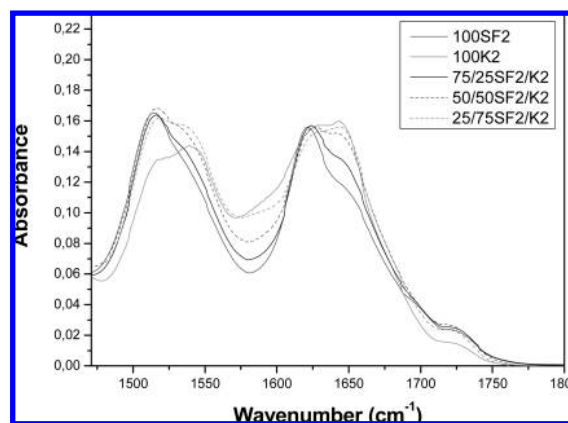
Figure 2. FTIR spectra of pure films of silk fibroin (SF1) and keratin (K1) aqueous solutions.
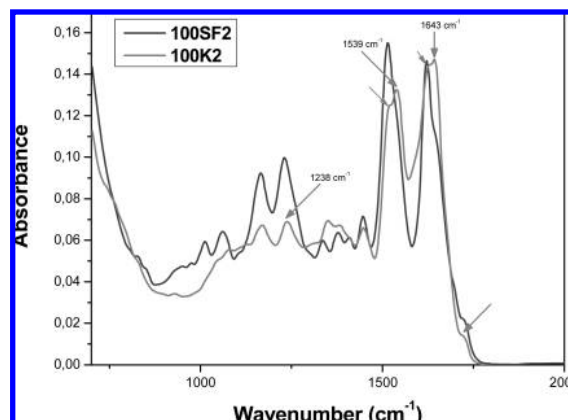
Figure 4. FTIR spectra of pure films of silk fibroin (SF2) and keratin (K2) dissolved in formic acid.
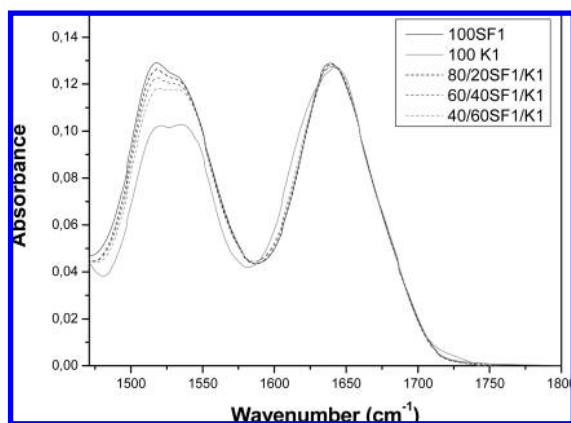
Figure 3. FTIR spectra of blended films with silk fibroin (SF1) and keratin (K1) aqueous solutions.

Figure 5. FTIR spectra of blended films with silk fibroin (SF2) and keratin (K2) dissolved in formic acid.

Figure 6. Behavior of intensity ratio of the amide II bands typical of SF1 (1518 cm^{-1}) and K1 (1533 cm^{-1}) in water and SF2 (1514 cm^{-1}) and K2 (1539 cm^{-1}) in formic acid.
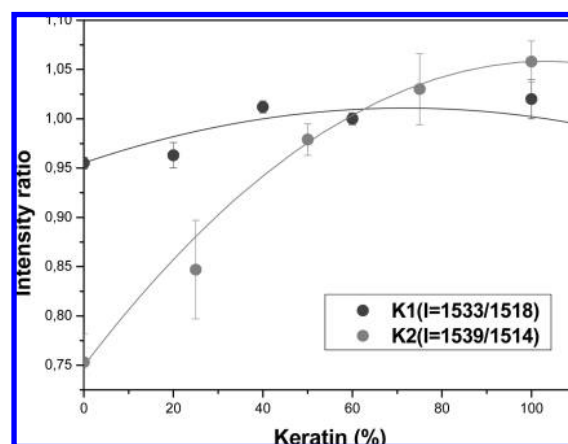
conformation). The half-peak width of amide I of K1 is larger than that of SF1, which might reflect a more heterogeneous molecular conformation.

Wool treatment with formic acid increases the amount of β-sheet and disordered keratin structures,[64,65] as it can be seen by the appearance of band peaks at the 1697–1670 cm^{-1} range in keratin dissolved in formic acid (K2, Figure 4).[59,66] Amide I at 1643 cm^{-1} with a strong shoulder at around 1620 cm^{-1}, amide II at 1539 cm^{-1} with a shoulder at about 1529 cm^{-1}, and amide III at 1238 cm^{-1}. The higher wavenumber of amide I can be explained by the protein extraction procedure suggesting again the presence of α-helix structure. Nevertheless, the decrease in the peak area of the amide I band in K2 spectra with respect to the same band in K1 spectra indicates that formic acid destabilized the α-helix conformation and stabilizes the supramolecular β-sheet structure of keratin. This occurs because formic acid has a higher polarity than water and forms strong interactions with the polar side chains groups of keratin. As a consequence, the molecular chains became closer and this organization can promote crystallization in β-sheet structure.[67]

The FTIR pattern of SF2 dissolved in formic acid is different from the one in water and characteristic of SF film with prevalently β-sheet conformation, with β-sheet crystallites embedded in an amorphous matrix.

Half-peak width of amide I and II of K2 are larger than those of SF2, suggesting a more heterogeneous molecular conformation as it was observed for aqueous solutions.

It can be observed (Figures 3 and 5) that the position, shape, and intensity of amide bands show a transition from an SF-like to a K-like spectral pattern, for both SF/K systems, with the increase of keratin present in the film. The plot of the intensity ratio between the amide II (Figure 6) bands fit a second-order polynomial curve, suggesting that SF and keratin do not follow additive rules when mixed. This might be indicating of intermolecular interactions, more likely hydrogen bonding, between SF and keratin.

3.4. DSC Results. The DSC curve of SF1 (Figure 7) exhibits an endothermic shift at 178 °C that corresponds to the glass-transition temperature (T_g) of SF, an exothermic peak at 226 °C (broad and weak) related to crystallization via conformational transition to β-sheet structure of amorphous SF chains, and an
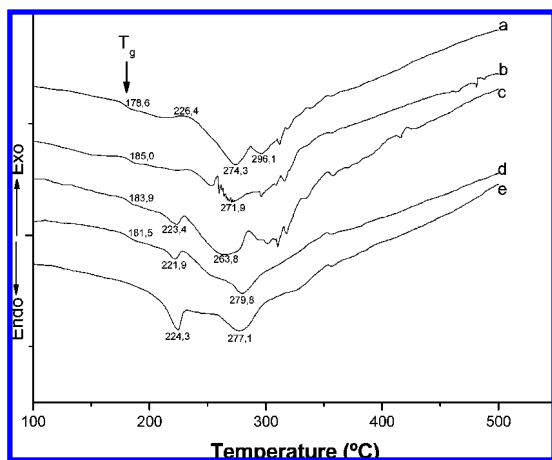
Figure 7. DSC curves of blended films with silk fibroin and keratin (SF1/K1) aqueous solutions: (a) 100SF, (b) 80/20SF1/K1, (c) 60/40SF1/K1, (d) 40/60SF1/K1, and (e) 100K1.
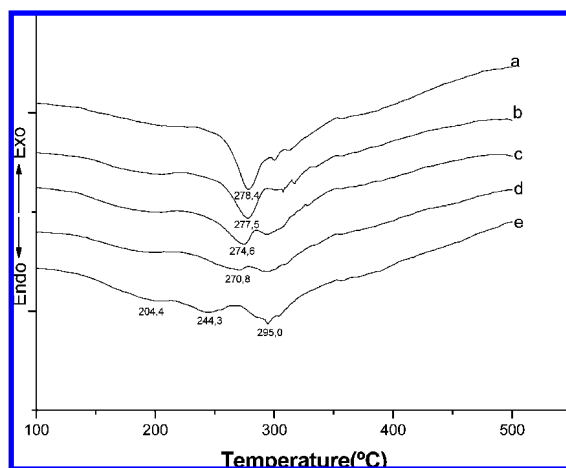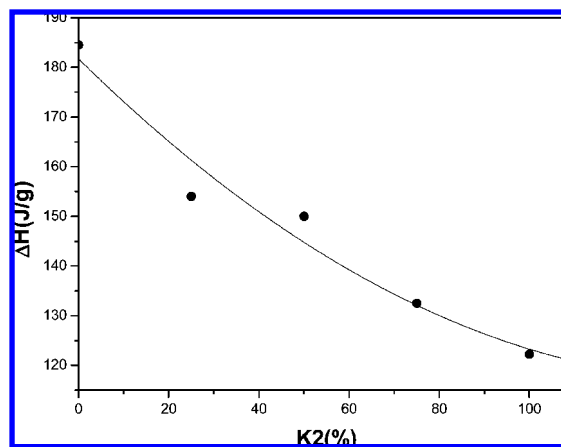

Figure 8. DSC curves of blended films with silk fibroin and keratin (SF2/K2) dissolved in formic acid: (a)100SF, (b) 75/25SF2/K2, (c) 50/50SF2/K2, (d) 25/75SF2/K2, and (e) 100K2.

Figure 9. ΔH of decomposition peak of SF2 and K2 (temperature range: 200–350 °C).

intense bimodal endotherm at 274 °C (main peak) and 296 °C assigned to the melting/decomposition of SF chains. The exothermic peak at 226 °C can be diminished by treatment with polar solvents[68] that was afterward observed (Figure 8). The thermal behavior is typical of a prevalently amorphous SF film with nonoriented SF chains. Weakness of the crystallization peak at 226 °C and presence of a high-temperature peak of thermal degradation at 296 °C suggest the presence of aggregated SF domains embedded in a prevalently amorphous matrix, as suggested by FTIR results.

The DSC curve of keratin (K1) (Figure 7) shows an endothermic peak at 224 °C related to the melting of α-helices of the intermediate filaments proteins and an endotherm peaking at 277 °C that corresponds to the melting/degradation of keratin associated proteins (KAPs) that comprise the high-sulfur (highly cross-linked) keratins of the intermacrofibrillar matrix.

The glass-transition temperature of SF1, T_g, shifts to higher temperature following addition of keratin. At higher keratin content (>60%), T_g is no more detectable. The melting peak of keratin α-helix at 224 °C remains almost unchanged; the value of ΔH (peak intensity) sharply decreases by addition of SF1. When 80% of SF1 is present in the blend, the melting peak of keratin is hardly detectable. The melting/decomposition endotherm of SF1 at 274 °C shows a marked low temperature broadening (the peak shifts downward of about 10 °C, from

274 °C to about 264 °C). It is still detectable in the 60% keratin blend as a low-temperature shoulder of the main keratin degradation endotherm. When silk fibroin (SF2) and keratin (K2) were dissolved in formic acid (Figure 8), the DSC pattern of both components changed. The glass-transition temperature and the exothermic peak of β-sheet crystallization are no more detectable because formic acid is able to induce a partial crystallization to β-sheet structures of SF chains during drying. The melting/decomposition endotherm of partially crystallized/nonoriented SF chains occurs at 278 °C with a high-temperature shoulder.

The DSC curve of keratin dissolved in formic acid (K2) is characterized by three main endothermic events at 204 °C (weak and broad), 244 °C, and the most intense at 295 °C. The transition at low temperature (204 °C) is hardly attributable and could be related to small molecular weight keratin fractions with low thermal stability. The thermal transitions peaking at 244 and 295 °C can be attributed to melting and melting/decomposition of keratin fractions with intermediate and high thermal stability, which is probably related to the different extent of cross-linking of the various keratin fractions. The characteristic α-helix melting peak of keratin is lost upon formic acid casting as already observed elsewhere.[67] This suggests that the α-crystallites formed by keratin/formic acid systems are thermally less stable. Furthermore, the peak area decrease (Figure 8) is a support of the lesser α-helix content in the K2 films. In the blends, the melting/decomposition endotherm of SF2 at 278 °C shifts to lower temperature with the increase of keratin present in the film. The energy associated with melting/decomposition of pure SF, pure keratin, and SF2/K2 blends was calculated by integrating the endothermic peaks in the range 200–350 °C (Figure 9). Values were expressed as ΔH (J/g). The energy associated with thermal degradation of SF2 is higher than that required by K2 (influence of the different chemical and physical structure). The plot of ΔH vs the composition of the blend does not follow a linear trend. The best fit is given by a second-order polynomial curve.

The nonlinear trend of the different parameters obtained from the DSC curves of both SF/keratin systems indicate that, when the proteins are mixed, the thermal behavior of one component is more or less strongly influenced by the other. This confirm the assumption raised by FTIR results that SF and keratin are able to establish intermolecular interactions, more likely based on hydrogen bonding.

3.5. In Vitro Degradation Results. In vitro degradation was observed for protein films of both SF/K systems incubated in
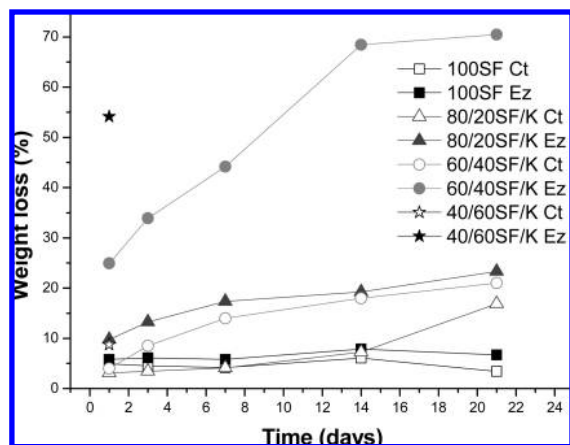
Figure 10. Weight loss of SF1/K1 films (water system) incubated in buffer (Ct) and trypsin solution (Ez) as a function of time.
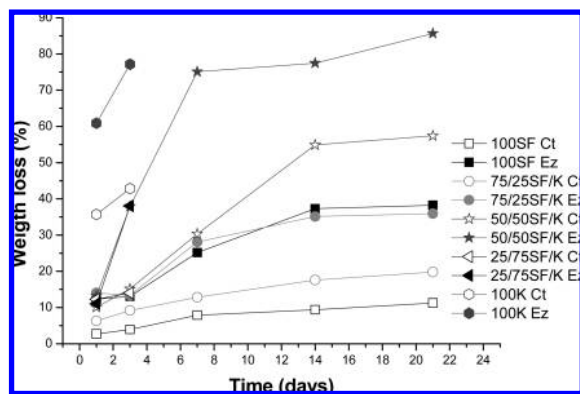

Figure 11. Weight loss of SF2/K2 films (formic acid system) incubated in buffer (Ct) and trypsin solution (Ez) as a function of time.

trypsin. In the water system (Figure 10), it can be observed that pure SF1 films presented very low degradation that remains constant over the time exposure to trypsin. In the blends, it can be seen that the weight loss obtained is a function of the amount of keratin (K1) present in the blend. When the minimum amount of K1 is present (20%), it obtained a degradation of 23% in a slow manner over the time. With the increase of keratin to 40%, the degradation took place rapidly during the first 14 days, remaining constant after that without exceeding 70% of degradation. At higher keratin amounts, only debris was obtained after 1 day of incubation.

In the formic acid SF2/K2 system (Figure 11), a similar behavior is observed. Nevertheless, pure SF films presented higher weight loss values, indicating that the crystallization to β-sheet, induced by formic acid of SF chains, make the amino acids more accessible for trypsin hydrolysis, increasing the degradation over the time.

4. Conclusions

In the present study, an extensive characterization of wool and silk proteins in the film form was presented. Films were made by blending silk fibroin (SF1) and keratin (K1) aqueous solutions and silk fibroin (SF2) and keratin (K2) dissolved in formic acid. The presence of K1 on the blends makes films weaker with a slight increase in elasticity, whereas films obtained from formic acid (SF2/K2) presented better strength results. The FTIR spectra of pure K1 indicates that its structure mainly consists of α-helix and random coil conformations. The IR spectrum of pure SF1 is characteristic of films with

prevalently amorphous structure (random coil conformation). Pure keratin film cast from formic acid (K2) show an increase in the amount of β-sheet and disordered keratin structures. The FTIR pattern of SF2 is characteristic of films with prevalently β-sheet conformation with β-sheet crystallites embedded in an amorphous matrix. In the blends, the position, shape, and intensity of amide bands show a transition from SF-like to K1-like or SF-like to K2-like spectral patterns. The thermal behavior of the blends confirmed the FTIR results. The DSC curve of pure SF is typical of amorphous SF, and the curve of pure K1 shows the characteristic melting peak of α-helixes. These patterns were no longer observed in the films cast from formic acid due to the ability of formic acid to induce crystallization of SF and to increase the amount of β-sheet structures on keratin.

The nonlinear trend of the different parameters obtained from FTIR analysis and DSC curves of both systems indicated that wool keratin and silk fibroin are able to establish intermolecular interactions. The properties of the films depend on the nature and strength of these interactions. The SF/K films cast from water underwent a slower biological degradation than the films cast from formic acid. The knowledge of the degradation rates will allow the design of matrices for the release of active compounds. The results presented show that the protein matrices developed are suitable to further biomedical and biotechnological applications.

References and Notes

(1) Feughelmann, M. In *Encyclopedia of Polymer Science and Engineering*, Vol. 8, Wiley: New York, 1985.
(2) Dowling, L. M.; Crewther, W. G.; Parry, D. A. D. *Biochem. J.* **1986**, *236*, 705–712.
(3) Plowman, J. E. *J. Chromatogr., B* **2003**, *787*, 63–76.
(4) Corey, R. B.; Pauling, L. *Wool Textile Research Conference*, Vol. B, Melbourne, Australia, 1956.
(5) Astbury, W. T.; Street, Phil, A. *Trans. R. Soc. London, A* **1931**, *230*, 75.
(6) Pauling, L.; Corey, R. *Nature* **1951**, *166*, 550.
(7) Pauling, L.; Corey, R. *Nature* **1953**, *171*, 59.
(8) Rhodes, H. J.; Potter, B.; Widra, A. *Mycropathol. Etmyclogia Appl.* **1967**, *33*, 345–348.
(9) Thomas, H.; Conrads, A.; Phan, K.-H.; van de Locht, M.; Zahn, H. *J. Biol. Macromol.* **1986**, *8*, 258–264.
(10) O'Donnell, I. J.; Thompson, E. O. P. *Aust. J. Biol. Sci.* **1964**, *17*, 973–979.
(11) Ito, M.; Tazawa, T.; Shimizu, N.; Ito, K.; Katsumi, K.; Sato, Y. *J. Invest. Dermatol.* **1988**, *86*, 563–569.
(12) Miyamoto, T.; Sakabe, H.; Inagaki, H. *Bull. Inst. Chem. Res.* **1987**, *65*, 109–119.
(13) Hayashi, R.; Kamei, K.; Kameda, T. Japanese Patent No. 9291138 (WPI C92-071192).
(14) Matsuda, H.; Takahashi, M.; Shinoda, S.; Kikyodani, S.; Inagaki, H. Japanese Patent 7842281, 1978; *Chem. Abstr.*, 1978, *89*, 76049f.
(15) Yamauchi, K. (a review 9291138 (WPI C92–071192), in Japanese), *Fragrance J.* **1993**, 62–67; *Chem. Abstr.* **1993**, *119*, 50734.
(16) Yamauchi, K.; Yamauchi, A.; Kusunoki, T.; Kohda, A.; Konishi, Y. *J. Biomed. Mater. Res.* **1996**, *31*, 439–444.
(17) Lee, K.; Kong, S.; Park, W.; Ha, W.; Kwon, I. *J. Biomater. Sci., Polym. Ed* **1998**, *9* (9), 905–914.
(18) Alemdar, A.; Iridag, Y.; Kazanci, M. *Int. J. Biol. Macromol.* **2005**, *35*, 151–153.
(19) Liu, Y.; Shao, Z.; Zhou, P.; Chen, X. *Polymer* **2004**, *45*, 7705–7710.
(20) Wong Po Foo, C.; Kaplan, D. L. *Adv. Drug. Delivery Rev.* **2002**, *54* (8), 1131–1143.
(21) Altman, G. H.; Diaz, F.; Jakuba, C.; Calabro, T.; Horan, R. L.; Chen, J.; Lu, H.; Richmond, J.; Kaplan, D. L. *Biomaterials* **2003**, *24* (3), 401–416.
(22) Arai, T.; Freddi, G.; Innocenti, R.; Tsukada, M. *J. Appl. Polym. Sci.* **2004**, *91*, 2383–2390.
(23) Fuchs, S.; Motta, A.; Migliaresi, C.; Kirkpatrick, C. J. *Biomaterials* **2006**, *27* (31), 5399–5408.

(24) Horan, R. L.; Antle, K.; Collette, A. L.; Wang, Y.; Huang, J.; Moreau, J. E.; Volloch, V.; Kaplan, D. L.; Altman, G. H. *Biomaterials* **2005**, *26* (17), 3385–3393.

(25) Hu, K.; Lv, Q.; Cui, F.; Feng, Q.; Kong, X.; Wang, H.; Huang, L. Y.; Li, T. *J. Bioactive Compatible Polym.* **2006**, *21* (1), 23–37.

(26) Karageorgiou, V.; Meinel, L.; Hofmann, S.; Malhotra, A.; Volloch, V.; Kaplan, D. *J. Biomed. Mater. Res. A* **2004**, *71* (3), 528–537.

(27) Kim, U. J.; Park, J.; Kim, H. J.; Wada, M.; Kaplan, D. L. *Biomaterials* **2005**, *26* (15), 2775–2785.

(28) Li, C.; Vepari, C.; Jin, H. J.; Kim, H. J.; Kaplan, D. L. *Biomaterials* **2006**, *27* (16), 3115–3124.

(29) Minoura, N.; Aiba, S.; Gotoh, Y.; Tsukada, M.; Imai, Y. *J. Biomed. Mater. Res.* **1995**, *29* (10), 1215–1221.

(30) Motta, A.; Migliaresi, C.; Faccioni, F.; Torricelli, P.; Fini, M.; Giardino, R. *J. Biomater. Sci., Polym. Ed.* **2004**, *15* (7), 851–864.

(31) Vepari, C. P.; Kaplan, D. L. *Biotechnol. Bioeng.* **2006**, *93* (6), 1130–1137.

(32) Arai, T.; Freddi, G.; Colonna, G. M.; Scotti, E.; Boschi, A.; Murakami, R.; Tsukada, M. *J. Appl. Polym. Sci.* **2001**, *80*, 297–303.

(33) Zhou, C. Z.; Confalonier, F.; Medina, N.; Zivanovic, Y.; Esnault, C.; Yang, T.; Jacquet, M.; Janin, J.; Duguet, M.; Perasso, R.; Li, Z.-G. *Nucleic Acids Res.* **2000**, *28* (12), 2413–2419.

(34) Kaplan, D. L., Mello, S. M., Arcidiacono, S., Fossey, S., Senecal K. W. M. In *Protein-Based Materials*; McGrath, K. K. D., Kaplan, D., Eds.; Birkhauser: Boston, 1998; pp 103–131.

(35) Yamaguchi, K.; Kikuchi, Y.; Takagi, T.; Kikuchi, A.; Oyama, F.; Shimura, K.; Mizuno, S. *J. Mol. Biol.* **1989**, *210* (1), 127–139.

(36) Inoue, S.; Tanaka, K.; Arisaka, F.; Kimura, S.; Ohtomo, K.; Mizuno, S. *J. Biol. Chem.* **2000**, *275* (51), 40517–40528.

(37) Lotz, B.; Colonna Cesari, F. *Biochimie* **1979**, *61*, 205–214.

(38) Yamauchi, K.; Yamauchi, A.; Kusunoki, T.; Kohda, A.; Konishi, Y. *J. Biomed. Mater. Res.* **1996**, *31*, 439–444.

(39) Tanabe, T.; Okitsu, N.; Tachibana, A.; Yamauchi, K. *Biomaterials* **2002**, *23*, 817–825.

(40) Minoura, N.; Tsukada, M.; Nagura, M. *Biomaterials* **1990**, *11*, 430.

(41) Minoura, N.; Tsukada, M.; Nagura, M. *Polymer* **1990**, *21*, 265.

(42) Tamada, Y.; Furuzono, T.; Taguchi, T.; Kishida, A.; Akashi, M. *J. Biomater. Sci., Polym. Ed.* **1999**, *10*, 787.

(43) Altman, G. H.; Horan, R. L.; Lu, H. H.; Moreau, J.; Martin, I.; Richmond, J.; Kaplan, D. L. *Biomaterials* **2002**, *23*, 4131.

(44) Furuzono, T.; Ishihara, K.; Nakabayashi, N.; Tamada, Y. *Biomaterials* **2000**, *21*, 327.

(45) Minoura, N.; Aiba, S.; Higuchi, M.; Gotoh, Y.; Tsukada, M.; Imai, Y. *Biochem. Biophys. Res. Commun.* **1995**, *208*, 511.

(46) Gotoh, Y.; Tsukada, M.; Minoura, M. *J. Biomed. Mater. Res.* **1998**, *39*, 351.

(47) Inouye, K.; Kurokawa, M.; Nishikawa, S.; Tsukada, M. *J. Biochem. Biophys. Methods* **1998**, *37*, 159.

(48) Sofia, S.; McCarthy, M. B.; Gronowicz, G.; Kaplan, D. L. *J. Biomed. Mater. Res.* **2001**, *54*, 139.

(49) Laemmli, U. K. *Nature* **1970**, *227*, 680.

(50) Thomas, H.; Conrads, A.; Phan, K.-H.; van de Locht, M.; Zahn, H. *lnt. J. Biol. Macromol.* **1986**, *8*, 258–264.

(51) Amiya, T.; Kajiwara, K.; Miyamoto, T.; Inagaki, H. *Int. J. Biol. Macromol.* **1982**, *4*, 165–172.

(52) Um, I. C.; Kweon, H. Y.; Lee, K. G.; Park, Y. H. *Int. J. Biol. Macromol.* **2003**, *33*, 203.

(53) Yamada, H.; Nakao, H.; Takasu, Y.; Tsubouchi, K. *Mater. Sci. Eng., C* **2001**, *14*, 41.

(54) MacLaren J. A.; Milligan, B. *Wool Science*; Science Press: Marrickville, NSW, 1981; Vol. 1, p 35.

(55) Katoh, K.; Shibayama, M.; Tanabe, T.; Yamauchi, K. *Biomaterials* **2004**, *25*, 2265–2272.

(56) Goo, H. C.; Hwang, Y.-S.; Choi, Y. R.; Cho, H. N.; Suh, H. *Biomaterials* **2003**, *24*, 5099.

(57) Tonin, C.; Aluigi, A.; Vineis, C.; Varesano, A.; Montarsolo, A.; Ferrero, F. *J. Therm. Anal. Calorim.* **2007**, *89* (2), 601–608.

(58) Zahn, H. *Int. J. Cosmet. Sci.* **2002**, *24*, 163–169.

(59) Wojciechowska, E.; Wlochowicz, A.; Weselucha-Birczynska, A. *J. Mol. Struct.* **1999**, *511–512*, 307–318.

(60) Bhat, N. V.; Ahirrao, S. M. *J. Polym. Sci., Polym. Chem.* **1983**, *21*, 1273.

(61) Ha, S. W.; Tonelli, A. E.; Hudson, S. M. *Biomacromolecules* **2005**, *6*, 1722.

(62) Tsukada, M.; Gotoh, Y.; Nagura, M.; Minoura, N.; Kasai, N.; Freddi, G. *J. Polym. Sci., Part B: Polym. Phys.* **1994**, *32*, 961.

(63) Berli, C. L. A.; Deiber, J. A.; Anon, M. C. *Food Hydrocolloids* **1999**, *13*, 507–515.

(64) Barone, J. R.; Schmidt, W. F. *Bioresour. Technol.* **2006**, *97*, 233–242.

(65) Pielesz, A.; Freeman, H. S.; Weselucha-Birczynska, A.; Wysocki, M.; Wlochowicz, A. *J. Mol. Struct.* **2003**, *651–653*, 405–418.

(66) Lyman, D. J.; Murray-Wijelath, J.; Feughelman, M. *Appl. Spectrosc.* **2001**, *55* (5), 552–554.

(67) Aluigi, A.; Zoccola, M.; Vineis, C.; Tonin, C.; Ferrero, F.; Canetti, M. *Int. J. Biol. Macromol.* **2007**, *41* (3), 266–273.

(68) Tsukada, M. *J. Polym. Sci., Part B: Polym. Phys.* **1986**, *24*, 1227.